

Study of aluminium oxide from high-alumina refractory ceramics by thermoluminescence

V CORRECHER, J GARCIA-GUINEA[†], R GONZALEZ-MARTIN[†], E CRESPO-FEO[†] and D JIMENEZ-CORDERO[†]

CIEMAT, Avda. Complutense 22, 28040 Madrid, Spain

[†]MNCN-CSIC, J. Gutierrez Abascal 2, 28006 Madrid, Spain

MS received 18 March 2008; revised 11 September 2008

Abstract. This work is focused on the study of the thermally stimulated blue emission of aluminium oxide (Al_2O_3) that has been removed from twenty different high alumina-rich refractory bricks. The glow curve sensitivity of several alumina grains are defined by (i) a maximum centred at about 165°C that can be deconvoluted into two first order kinetic peaks at 157 and 177°C and (ii) a broad structure over 200 – 220°C that suggests a continuous trap distribution system. The isolated grains, analysed by means of X-ray diffraction, are composed of 43% of alumina (Al_2O_3), 22% of mullite [72% of Al_2O_3 and 28% of SiO_2], 12% of leucite (KAlSi_2O_6) and 23% of sillimanite [Al_2O_3 - SiO_2]. The sample characterization has been performed using X-ray fluorescence and scanning electron microscopy.

Keywords. Ceramics; aluminium oxide; X-ray diffraction; scanning electron microscopy; thermoluminescence.

1. Introduction

The studies performed on the thermomechanical properties and the microstructure of synthetic alumina (Al_2O_3) have been widely investigated (Mitra *et al* 1992). In this sense, synthetic Al_2O_3 obtained by Verneuil (Manuilov and Peshev 1992), Bayer process (Mahadevan and Ramachandran 1996) or Czochralski (Baughman and Lefever 1975) method, doped with different types and proportion of impurities, have been of great interest not only for industrial purposes, but also to be employed in the field of thermoluminescence (TL) dosimetry (Molnar *et al* 1999; Tokumoto *et al* 2006).

The TL emission of ceramic materials and mineral phases concerns inter-disciplinary research areas involving both solid-state physics and radiation physics with wide-ranging applications in geological (Bailey 2004) and archaeological (Feathers 2003) dating, retrospective assessment of irradiation dose (Pandya *et al* 2000; Bailiff *et al* 2005) and detection of irradiated food (Correcher *et al* 1998). These ubiquitous materials appear as a reasonable alternative to the conventional dosimetric systems since they have good sensitivity to radiation, a linear response with the increase of dose and reasonable stability of the luminescence signal with the time of storage (Correcher *et al* 2004). This behaviour has been used for the dose

evaluation in several retrospective dosimetry studies based on luminescence techniques usually performed on quartz removed from common ceramic materials. Such methodology has been successfully applied with traditional red clay bricks and tiles to estimate the cumulative external gamma dose arising from the radiation of Chernobyl accident (Bailiff *et al* 2005) and tentatively in cements (Gartia *et al* 1995). However, one can consider the possibility of using alternative ceramic materials for dosimetric purposes, e.g. high-alumina rich refractory bricks since they (i) could exhibit luminescence properties similar to the well-known synthetic alumina (α - Al_2O_3) and (ii) have been annealed and, consequently, the thermoluminescence (TL) clock has been properly set to zero. These materials that have been seldom investigated for such purposes are characterized by the lack of quartz owing to a chemical reaction that produces mullite ($\text{Al}_2\text{O}_3 + \text{SiO}_2 \rightarrow \text{Al}_2\text{SiO}_5$) (Tripathi *et al* 2003). On this basis, it could be expected that the TL behaviour of synthetic alumina grown under controlled conditions does not differ too much from aluminium oxide extracted from the alumina rich refractory bricks. The crystal structure of alumina, which is found in nature as corundum, sapphire and ruby, consists of a slightly distorted hexagonal O^{2-} ion sub-lattice (C_2 symmetry) with Al^{3+} ions in two out of three octahedral interstices (O_h symmetry). The unit cell symmetry is C_3 (Tokumoto *et al* 2006). Two electrons giving rise to a neutral F centre occupy each oxygen vacancy centre. When F^+ centre is formed (i.e. occupancy

*Author for correspondence (v.correcher@ciemat.es)

of one instead of two electrons), compensators are required to preserve the charge balance of the lattice (Molnar *et al* 1999). These charge compensators can induce (i) the formation of defects in the structure, (ii) point defects, including aluminium-associated trapped hole centres and (iii) oxygen vacancies. All of them are directly related to the intensity and shape of the TL glow emission.

This paper reports on the characterization of TL of Al_2O_3 detected in the blue transmission band 320–480 nm from grains removed from high-alumina refractory bricks produced in an early 20th century metallurgical furnace in Hiendelaencina (Guadalajara, Spain) under reducing conditions. The samples were previously studied by means of X-ray diffraction (XRD), scanning electron microscopy (SEM) and X-ray fluorescence (XRF) to determine the structure and chemical content of impurities.

2. Experimental

All the brick samples were taken at a height of 1 m above ground level. Once in the laboratory, the twenty selected refractory bricks were cut using a water-lubricated diamond blade to produce different slices (figure 1) under red light to avoid the release of the trapped electrons from the metastable sites into hole centres by the environmental light irradiation. The white crystalline mineral grains, directly removed from the slices using mechanical crushing and sieving procedures, were analysed by means of XRD using the powder method in a Siemens D-5000 automated diffractometer with CuK_α radiation. The XRD measurements were performed by step scanning from 2°



Figure 1. Slice of one of the twenty analysed refractory bricks cut using a water-lubricated diamond blade.

to $64^\circ 2\theta$ in steps of 0.020° , and a counting time of 6 s per step. The chemical composition of these white grains has been analysed by XRF. A pressed pill of powdered samples weighing 8 g was chemically analysed by wavelength XRF to determine its global chemical composition in major and trace elements at the $\mu\text{g}\cdot\text{g}^{-1}$ level. Both, qualitative and quantitative measurements were performed in an XRF-spectrometer PW-1404 Philips, equipped with an X-ray tube of Sc–Mo, a scintillation crystal detector Harshaw type NaI(Tl) and operating at 80 kW and 30 mA. SEM assays were done using a Zeiss DSM-90 (40 kV electron microscope with a resolution of 70 Å). The micro-analysis detector was a Si–Li model, using a Tractor Northern Z2 computer. Sample metallization were made using gold vapour in a vacuum (50 Å of gold cover).

The TL measurements were performed using an automated Risø TL system model TL DA-12 (Botter-Jensen and Duller 1992), this reader has an EMI 9635 QA photomultiplier and the emission was observed through a blue filter (FIB002 Melles-Griot) with transmission in the 320–480 nm range; FWHM is 80 ± 16 nm and peak transmittance is 60%. It has a $^{90}\text{Sr}/^{90}\text{Y}$ beta source with a dose rate of 0.020 Gy s^{-1} calibrated against a ^{60}Co photon source in a secondary standards laboratory (Correcher and Delgado 1998). The TL measurements were performed at a heating rate of $5^\circ\text{C}\cdot\text{s}^{-1}$ from room temperature to 500°C in a N_2 atmosphere. A set of four aliquots of 5 ± 0.1 mg each of the sample was used for each measurement. The sample was carefully powdered (90–125 μm) with a pestle and mortar to avoid triboluminescence (Garcia-Guinea and Correcher 2000). The incandescent background was subtracted from the TL data. The kinetic parameters of the TL glow peaks were estimated by means of a computerized curve-fitting program based on first order kinetics, glow curve analysis (GCA), developed by Delgado and Ros (2001) that allows the identification of the TL glow curve structure.

3. Results and discussion

3.1 Sample characterization

According to the XRD study, the main composition of the white grains removed from the whole refractory bricks is: 43% of corundum (Al_2O_3), 22% of mullite [72% of Al_2O_3 and 28% of SiO_2], 12% of leucite (KAlSi_2O_6) and 23% of sillimanite [$\text{Al}_2\text{O}_3\cdot\text{SiO}_2$] (figure 2). The isolated grains of white pure alumina [Al_2O_3], embedded in a mullite matrix, allow us to speculate that the starting raw material to produce the bricks, is mainly made of a mixture of previously ground pure alumina sand together with kaolinite [$\text{Al}_2\text{Si}_2\text{O}_5(\text{OH})_4$]. These bricks were probably processed by moulding under high pressure and sintering under high temperature, with features like large heat accumulating capacity and small creep rate. Such a mixture, melted during the refractory brick firing, gave rise to sillimanite

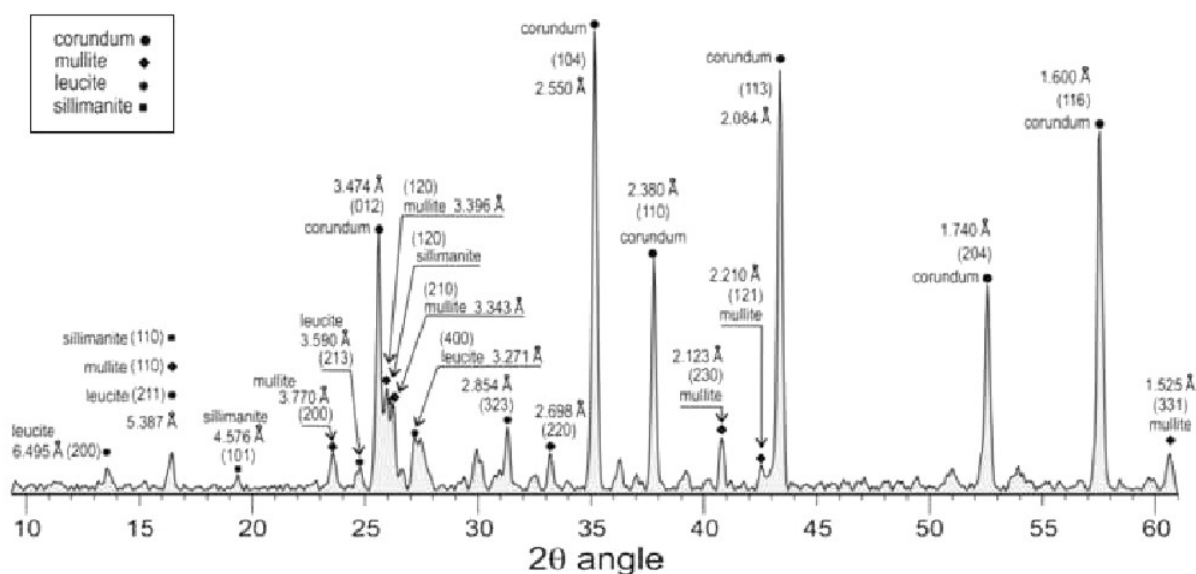


Figure 2. X-ray diffractogram performed on a white opaque grain. It is possible to distinguish 43% of corundum (Al_2O_3), 22% of mullite [72% of Al_2O_3 and 28% of SiO_2], 12% of leucite (KAlSi_2O_6) and 23% of sillimanite [$\text{Al}_2\text{O}_3 \cdot \text{SiO}_2$].

and leucite. All the detected components could act as natural phosphors for dosimetric purposes since they exhibit luminescence emission (Wojtowicz and Lempicki 1989; Yarovoi and Veksler 1998; Garcia-Guinea *et al* 2001a).

The SEM observations indicate the presence of a fine layer of ZrO_2 on the surface of several alumina grains (figure 3). It probably stems from zircon [ZrSiO_4] rich natural mixed sands usually employed in the brick production. It is quite common to find small amounts of different natural radioactive impurities (U and Th) in zircon compounds that are the suppliers of radiation energy necessary to induce TL emission.

The bulk chemical analysis of the alumina samples, performed under XRF, indicates the presence of Fe (2120 ppm), Ti (1580 ppm), K (1190 ppm), Zr (862 ppm), Ca (680 ppm), Na (550 ppm), Ba (386 ppm), Mg (320 ppm), Zn (236 ppm), Sr (227 ppm), Pb (169 ppm) and Cu (138 ppm). These impurities, especially trivalent ions (Fe^{3+}), substitute the Al in the whole framework and all valence bonds are satisfied. However, when divalent cations (Mg^{2+} , Ca^{2+} , Sr^{2+}) substitute the Al, interstitial monovalent ions (Na^+ , K^+) are required to preserve charge balance. The impurities that are incorporated into the alumina structure, yield intrinsic defects in the crystal lattice and will modify not only the relative intensity of component bands, but also changes in the wavelength response, quantum efficiency, temperature position in the TL signal and/or even induce new luminescence signals. Such behaviour is a consequence of the lattice distortion due to the size of the incorporated impurities. We could not detect the radioactive impurities, using XRF, mainly due to the low concentration of the aforementioned acti-

nides (lower than detection limit of the equipment) that, according to previous studies performed on natural zircons, should be circa 6 ppb (Correcher *et al* 2003a).

3.2 Thermally stimulated luminescence

The natural TL glow curves show the appearance of two peaks at about 157 and 177°C, which is characteristic of materials containing Al–O bonds, and (above 200–220°C) a very complex structure consisting of a broad distribution typically observed in several natural materials (such as diaspor, an aluminium oxo-hydroxide $-\alpha\text{-AlOOH}-$) (Correcher *et al* 2003b). The TL physical trapping parameters for the curve (trap depth in eV, E , frequency factor in s^{-1} , s , intensity of the maximum in arbitrary units, a.u., I_{max} , peak position in °C, T_{max} , and figure of merit in percentage (FOM), parameter that indicates the goodness of the fitting) were estimated using the GCA program. All the analysed parameters were refined to a confidence limit of 95% accuracy. As shown in figure 4, the dashed lines correspond to the calculated fitted first order kinetics peaks, which make up the calculated fitted solid line. This encircling line is directly compared with the experimental dotted line.

The low-temperature peak (at 157°C) has also been detected in synthetic doped alumina ($\alpha\text{-Al}_2\text{O}_3$) (Molnar *et al* 1999). This maximum could be due to radiative decay F centres produced by the reduction of this material that leads to the formation of oxygen vacancies (F type centres) that would act as emission centres. According to Molnar *et al* (1999), the trap responsible of this maximum could be associated with Al^{3+} vacancies linked to

charge compensators, for example, oxygen vacancies giving rise to a complex defect (i.e. an electron trap). In an oxidizing atmosphere the oxygen vacancy concentration is reduced and, consequently, should decrease the recombination centres. This is probably the reason of the low level TL intensity observed in our samples. Assuming that the trap responsible for the 157°C peak in alumina is an electron trap, one could analyse the TL glow peak, as a good approach; in terms of first order kinetics (i.e. the intensity of the TL signal is proportional to the concentration of thermally released charges).

As observed in natural diaspore, the high-temperature maximum peaking at 177°C can be linked to a discrete trap structure (Garcia-Guinea *et al* 2001b, 2005). This peak has also been detected in $\text{Al}_2\text{O}_3:\text{C}$ that is usually employed for the estimation of environmental doses (Guissi *et al* 1999; Yukihiro *et al* 2003) and in natural diaspore (Correcher *et al* 2003b). It happens despite (i) this TL emission stems from aluminium oxide instead of diaspore, which possesses a different structure and (ii) its origin formed initially in oxidizing atmosphere and subsequently maintained in depleted oxygen atmosphere. Following the similar reasoning given for diaspore and synthetic alumina, this peak could be considered mainly associated with the presence of divalent impurities (e.g. Mg^{2+}) that replace Al^{3+} ; it supposes the generation of oxygen vacancies, which can act as recombination centres. Therefore, it could be accepted that the intensity of this emission is proportional to the concentration of traps given by the presence of different types or the concentration of divalent impurities. Both the value of activation energy and the frequency factor (s), that informs the probability per second for the release of a trapped charge

carrier of the experimental TL spectra, are well correlated with the theoretical calculations made by Guissi *et al* (1999) and Correcher *et al* (2003b) corresponding to alpha alumina and diaspore, respectively (table 1). The value of the FOM is lower than 4% that indicates an acceptable good fitting (Balian and Eddy 1977). The ratio of the TL intensities of both deconvoluted peaks, separated by 20°C, is $\sim 2:1$. Assuming the aforementioned interpretation, one can speculate that these samples possess a double number of electron trap centres (due to Al-vacancies compensated with oxygen vacancies) than Al-vacancies compensated with Mg impurities and oxygen vacancies that should act as recombination centres. On this basis, this ratio could be linked to two stages during the formation of the sample: (i) A process that should be associated with the synthesis of the corundum generated in oxidizing atmosphere during the sintering of the refractory brick. This process is related to a local disorder in the material and therefore, with the low-temperature TL signal. (ii) A low temperature treatment in reducing conditions produced during the working period of the bricks in the kiln that promote other defects producing the 177°C TL signal.

The low intensity broad structure over 200–220°C suggests a continuous trap distribution system as described in diaspore by Garcia-Guinea *et al* (2001b, 2005). It should correspond to de-hydroxylation mechanisms and chromophore oxidation that could help to explain the high temperature UV-blue emissions mainly due to the presence of leucite, sillimanite and mullite (figure 2). This thermolabile high temperature TL broad band of blue emission exhibits the typical multi-order kinetics behaviour involving continuous processes of electron trapping–detrapping. These thermal phenomena of TL are

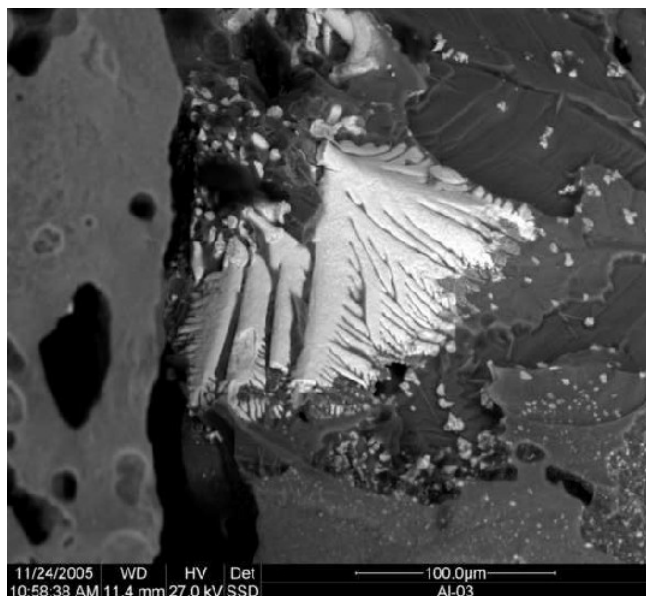


Figure 3. Detail of a SEM picture where ZrO_2 is observed on the surface of some alumina grains.

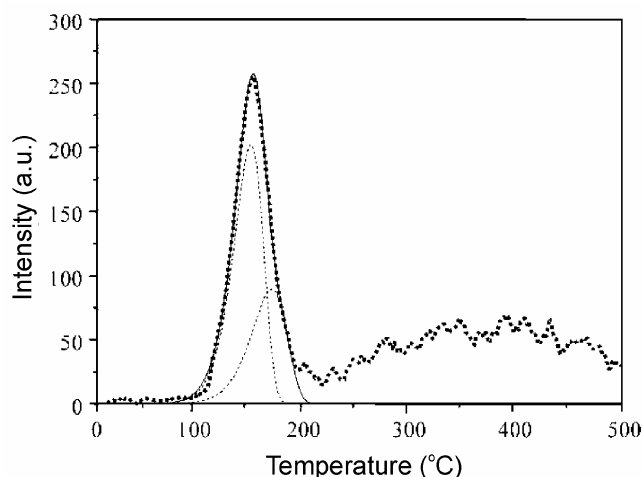


Figure 4. Natural TL glow curve of alumina removed from the refractory brick. The well-defined peak at lower temperature can be deconvoluted into two components (peaked at 157 and 177°C) assuming first order kinetics.

Table 1. Kinetic parameters resulting from the analysis of the natural TL glow curves of alumina removed from the refractory brick assuming first order kinetics. The value of the FOM (figure of merit) is 3.1%.

Peak	E (eV)	s (s^{-1})	I_{\max} (a.u.)	T_{\max} ($^{\circ}\text{C}$)	Area (%)
1	1.11 ± 0.02	3.71×10^{14}	202 ± 52	157 ± 4	65.41
2	1.01 ± 0.02	5.94×10^{12}	89 ± 21	177 ± 6	34.59

synchronous with the de-hydroxylation process, which carry out consecutive breaking linking of bonds of Al–O, Fe–O, Al–OH and Fe–OH including the formation of hydrolyzed ions such as $\text{Al}(\text{H}_2\text{O})_6^{3+}$, and $\text{Fe}(\text{H}_2\text{O})_6^{3+}$ and redox reactions; whereas there are some other non hydrolyzable chains that remain unchangeable (Guissi *et al* 1999; Garcia-Guinea *et al* 2005). In addition, the intrinsic structure of these specimens (leucite, sillimanite and mullite) includes twinning planes, antiphase domain boundaries, exsolution borders, modulations, etc. These natural superlattices complexity give many different points of egress for the alkali ions during thermal treatments; many distinct sets of dynamic TL traps are produced which could explain the difficulty in parametrizing the TL glow curves of the alkali aluminosilicates.

4. Conclusions

Grains of aluminium oxide removed from high alumina rich refractory bricks from an old and abandoned 20th century metallurgical furnace characterized by X-ray diffraction indicates that it is composed of 43% of alumina (Al_2O_3), 22% of mullite [72% of Al_2O_3 and 28% of SiO_2], 12% of leucite (KAlSi_2O_6) and 23% of sillimanite [$\text{Al}_2\text{O}_3 \cdot \text{SiO}_2$]. The blue TL emission of these Al_2O_3 grains exhibits two peaks at about 157 and 177 $^{\circ}\text{C}$, which is characteristic of materials containing Al–O bonds, and could be respectively linked to (i) Al-vacancies compensated with oxygen vacancies and (ii) Al-vacancies compensated with Mg impurities and oxygen vacancies that should act as recombination centres. At higher temperatures (above 200–220 $^{\circ}\text{C}$) it is possible to distinguish a very complex structure consisting of a wide distribution that could be associated with a continuous trap distribution due to the presence of leucite, sillimanite and mullite. The studied luminescent properties of this material show that it could be a potentially valid radiation environmental dosimeter to be applied in the field of geological dating or retrospective dosimetry as an alternative or complement of quartz, usually employed for these purposes.

Acknowledgements

This work has been supported by the CICYT (FIS2007-61823) and Comunidad Autonoma de Madrid (CAM)

MATERNAS (S-0505/MAT/0094) projects. Authors thank Dr Delgado and Dr Gomez-Ros for the GCA program.

References

- Bailey R M 2004 *Radiat. Meas.* **38** 299
 Bailiff I K *et al* 2005 *Health Phys.* **89** 233
 Balian H G and Eddy N W 1977 *Nucl. Instrum. Meth.* **145** 389
 Baughman R J and Lefever R A 1975 *Mater. Res. Bull.* **10** 607
 Botter-Jensen L and Duller G A T 1992 *Nucl. Track Radiat. Meas.* **20** 549
 Correcher V and Delgado A 1998 *Radiat. Meas.* **29** 411
 Correcher V, Muniz J L and Gomez-Ros J M 1998 *J. Sci. Food Agric.* **76** 149
 Correcher V, Robredo L M, Valle-Fuentes F J, Lopez-Arce P and Garcia-Guinea J 2003a *Bol. Soc. Esp. Ceram.* **42** 369
 Correcher V, Garcia-Guinea J and Valle-Fuentes F J 2003b *Geophys. Res. Lett.* **30** 1949
 Correcher V, Gomez-Ros J M and Garcia-Guinea J 2004 *Radiat. Meas.* **38** 689
 Delgado A and Ros J M G 2001 *Radiat. Prot. Dosim.* **96** 127
 Feathers J K 2003 *Meas. Sci. Technol.* **14** 1493
 Garcia-Guinea J and Correcher V 2000 *Spectrosc. Lett.* **33** 103
 Garcia-Guinea J, Correcher V and Rodriguez-Badiola E 2001a *Analyst* **126** 911
 Garcia-Guinea J, Rubio J, Correcher V and Valle-Fuentes F J 2001b *Radiat. Meas.* **33** 653
 Garcia-Guinea J, Correcher V, Rubio J and Valle-Fuentes F J 2005 *J. Phys. Chem. Solids* **66** 1220
 Gartia R K, Ingotombi S and Singh S D B 1995 *Mater. Sci.* **18** 107
 Guissi S, Iacconi P, Bindi R and Lapraz D 1999 *Radiat. Prot. Dosim.* **84** 247
 Mahadevan H and Ramachandran T R 1996 *Bull. Mater. Sci.* **19** 905
 Manuilov N and Peshev P 1992 *Mater. Res. Bull.* **27** 805
 Mitra B L, Biswas N C and Aggarwal P S 1992 *Bull. Mater. Sci.* **15** 131
 Molnar G, Papin E, Grosseau P, Guilhot B, Borossay J, Benabdesselam M, Iacconi P and Lapraz D 1999 *Radiat. Prot. Dosim.* **84** 253
 Pandya A, Vajapurkar S G and Bhatnagar P K 2000 *Bull. Mater. Sci.* **23** 155
 Tokumoto Y, Sato Y, Yamamoto T, Shibata N and Ikuhara Y 2006 *J. Mater. Sci.* **41** 2553
 Tripathi H S, Mukherjee B, Das S K, Ghosh A and Banerjee G 2003 *Bull. Mater. Sci.* **26** 217
 Wojtowicz A J and Lempicki A 1989 *Phys. Rev.* **B39** 8695
 Yarovi P N and Veksler A S 1998 *Inorg. Mater.* **34** 1149
 Yukihara E G, Whitley V H, Polf J C, Klein D M, McKeever S W S, Akselrod A E and Akselrod M S 2003 *Radiat. Meas.* **37** 627